Neuropsychologia 49 (2011) 3484–3493

Contents lists available at SciVerse ScienceDirect

Neuropsychologia

journal homepage: www.elsevier.com/locate/neuropsychologia

On the role of fronto-striatal neural synchronization processes for response inhibition—Evidence from ERP phase-synchronization analyses in pre-manifest Huntington's disease gene mutation carriers

Christian Beste[a,*], Vanessa Ness[a], Michael Falkenstein[b], Carsten Saft[c]

[a] Institute for Cognitive Neuroscience, Department of Biopsychology, Ruhr-University Bochum, Universitätsstrasse 150, D-44780 Bochum, Germany
[b] Leibniz Research Centre Dortmund, Aging and CNS Diseases, Germany
[c] Department of Neurology, Huntington Centre NRW, St. Josef Hospital, Ruhr-University Bochum, Germany

ARTICLE INFO

Article history:
Received 21 June 2011
Received in revised form 15 August 2011
Accepted 24 August 2011
Available online 1 September 2011

Keywords:
Response inhibition
Huntington's disease
Compatibility effects
Neural synchronization
Event-related potentials (ERPs)

ABSTRACT

Fronto-striatal loops play an important role action selection processes, especially when discordant sensory and contextual information has to be integrated to allow adequate selection of actions. Neurodegeneration weakens neural inter-connectivity, which compromises the precision of neural synchronization processes. Yet, it is widely unknown how far changes in the precision of neural synchronization processes are induced by only slight dysfunctions of striatal neural inter-connectivity and in how far such slight changes may affect action selection processes.

We investigated these processes in a sample of 25 pre-HDs and case-matched controls in a modified Go/Nogo task, while assessing neural synchronization processes by means of phase-locking factors (PLFs) as derived from event-related potentials (ERPs).

The results show that pre-HDs only encounter problems in response inhibition, when discordant contextual information and sensory input have to be integrated. No deficits were evident, when response inhibition can be based on more habitual stimulus–response mappings, i.e., when contextual and sensory information were congruent. While 'habitual' action selection is unaffected by changes in striatal structures influencing reliability of neural synchronization processes, efficient 'controlled' processes of action seem to be closely dependent upon highly reliable neural synchronization processes. The neurophysiological analysis suggests that especially pre-motor inhibition processes (Nogo-N2) are affected. This was most strongly reflected in a decline in the degree of phase-locking in the Nogo-N2 range. Deficits in pre-HDs seem to emerge as a consequence of phase-locking-behavioural decoupling. Of clinical interest, declines in the precision of phase-locking depended on the amount of the individual's mutant huntingtin exposure and predicted the probability of disease manifestation in the next five years. This suggests that phase-locking parameters may prove useful in future studies evaluating a possible function as a biomarker in Huntington's disease.

© 2011 Elsevier Ltd. All rights reserved.

1. Introduction

Cortico-striatal loops mediate several cognitive processes related to the inhibition and selection of actions (DeLong & Wichmann, 2007). To investigate the relevance of fronto-striatal loops for cognitive processes the examination patients suffering under degenerative basal ganglia disease provide insights into the basal ganglia mechanisms that mediate specific cognitive processes. Fronto-striatal loops are early affected in Huntington's disease (HD), an autosomal, dominant neurological disorder caused by an extension of the CAG-repeat length at the 4th chromosome (Huntington's Disease Collaborative Research Group, 1993). Neurodegeneration starts in the striatum and is evident before motor symptoms of disease become manifest (i.e., pre-manifest HD; pre-HD) (e.g. Rosas et al., 2008; Tabrizi et al., 2009). In these early disease stages, neurodegeneration compromises the inter-connectivity of striatal medium-sized spiny neurons (MSNs) (e.g. Cepeda, Wu, Andre, Cummings, & Levine, 2007; Mitchell, Cooper, & Griffith, 1999; Tabrizi et al., 2009).

Even though it is well-known that degraded neural inter-connectivity compromises the efficacy and precision of neural synchronization (Kitano & Fukai, 2004; Lago-Fernandez, Corbacho, & Huerta, 2001), it is unknown how far changes in the precision of neural synchronization processes are induced by only slight dysfunctions of striatal neural inter-connectivity and in how far such slight changes may affect action selection processes.

* Corresponding author. Tel.: +49 234 322 4323; fax: +49 234 321 4377.
E-mail address: christian.beste@rub.de (C. Beste).

0028-3932/$ – see front matter © 2011 Elsevier Ltd. All rights reserved.
doi:10.1016/j.neuropsychologia.2011.08.024

Action selection requires the integration of sensory inputs with contextual information (e.g. Bar-Gad, Morris, & Bergman, 2003; Gurney, Prescott, Wickens, & Redgrave, 2004; Redgrave & Gurney, 2006). This integration is especially important when habitual action control is not adequate and controlled processes have to operate to allow adequate action selection (Redgrave et al., 2010). Action selection processes can be examined using Go/Nogo tasks. Due to the early cortico-striatal dysfunctions in HD, even pre-manifest Huntington's disease gene mutation carriers (pre-HDs) may not able to integrate sensory inputs with contextual information to select the appropriate actions.

Event-related potentials (ERPs) reliably reflect different subprocesses of response inhibition in basal ganglia diseases (e.g. Beste, Saft, Andrich, Gold, & Falkenstein, 2008a; Bokura, Yamaguchi, & Kobayashi, 2005; Praamstra & Plat, 2001) that relate to the inhibition or revision of a motor plan/program before the actual motor process (i.e., Nogo-N2), or the monitoring of the outcome of inhibition (i.e., Nogo-P3) (see: Band & van Boxtel, 1999; Beste, Baune, Domschke, Falkenstein, & Konrad, 2010a; Beste, Willemssen, Saft, & Falkenstein, 2010; Nieuwenhuis, Yeung, van den Wildenberg, & Ridderinkhof, 2003; Roche, Garavan, Foxe, & O'Mara, 2005). It has previously been shown that response inhibition processes are dysfunctions in manifest HD, but not in pre-manifest HD (Beste, Willemssen, et al, 2010; Beste et al., 2008a), when habitual stimulus–response mappings underly action selection in a Go/Nogo task. However, when one context requires the opposite stimulus–response mapping than the previous context, the contextual information interferes with previously strengthened, possibly habitual stimulus–response mappings and compromises response inhibition processes. Under such conditions, we hypothesize that fronto-striatal circuits may become overstrained even in the pre-manifest phase of HD, which leads dysfunctions in response inhibition and to a decline in the rate of correct rejections. As especially response inhibition processes and the revision of a motor plan/program are more demanded in such conditions (see: Beste, Dziobek, Hielscher, Willemssen, & Falkenstein, 2009), these effects should be reflected in the Nogo-N2 ERP component. The Nogo-N2 should be attenuated in pre-manifest Huntington's disease gene mutation carriers (pre-HDs).

On the basis of these ERPs, we further examine properties of neural synchronization processes by means of phase-locking factors (PLFs) (Beste, Kolev, et al., 2010; Roach & Mathalon, 2008; Tallon-Baudry, Bertrand, & Fischer, 2001). A high phase-locking factor (PLF) indicates that neural synchronization, or phase-synchrony is precise or reliable in time and frequency, while a low PLF indicates that timing and frequency of neural synchronization across trials is less reliable (Roach & Mathalon, 2008). For the phase-locking analysis we hypothesize that timing and frequency of neural synchronization is less reliable, when pre-HDs have to integrate discordant contextual and sensory information to perform response inhibition. These phase-locking deficits are expected to determine response inhibition deficits in this condition. As these deficits are most likely determined by severity of neurodegeneration in pre-HDs, we expect that the individual's decline in phase-locking is related to the individual's mutant huntingtin exposure (Penney, Vonsattel, MacDonald, Gusella, & Myers, 1997; Tabrizi et al., 2009) and also on the probability to enter the symptomatic stage within a certain time period (Langbehn, Brinkman, Falush, Paulsen, & Hayden, 2004).

2. Materials and methods

2.1. Participants

A group of 25 right-handed, pre-manifest HD gene mutation carriers (pre-HDs) defined by a positive gene test and absence of clinical motor symptoms were recruited. Classification as "absence of clinical motor symptoms" was based on expert raters' assessments of motor signs which were not sufficient for the diagnosis of HD (Diagnostic Confidence Level [DCL], item 17 of the UHDRS Motor Assessment) (Huntington Study Group, 1996). All HD participants underwent neurological investigation and were scored according to the UHDRS items "motor scale" (MS), "total functional capacity" (TFC) "independence scale" (IS) and the items verbal fluency test, symbol digit test, interference test, colour naming and word reading which were summarized as "cognitive score" (CS) (Huntington Study Group, 1996). For each pre-manifest participant the probability of estimated disease onset (Age of onset; AO) within 5 years was calculated according to Langbehn et al.'s parametric model (Langbehn et al., 2004). Also the expected AO was estimated using the Langbehn's formula. Years to disease onset (YTO) for the pre-HD subjects were calculated by subtracting the subject's age at the time of investigation from his or her estimated onset age. The YTO for each subject were used to dichotomize pre-manifest HD group into carriers close to estimated age of onset [cEAO] and far from estimated age of onset [fEAO]) (e.g. Tabrizi et al., 2009), by median-split. We also calculated the "Disease burden score" (DBS = [CAG repeat − 35.5] × age) for each subject (e.g. Penney et al., 1997; Tabrizi et al., 2009). None of the mutation carriers was on medication (except one timipramine 50 mg and one fluoxetine 20 mg).

As controls, a group of 25 right-handed, healthy subjects matched to the pre-HD group in age, sex, educational status and socio-economic background was enrolled in the study. All participants gave written informed consent, before any of the study protocols were commenced. The demographical information is given in Table 1.

The study was approved by the Ethics Committee of the Ruhr-University Bochum, Germany. The study was conducted according to the Declaration of Helsinky.

2.2. Task

We used a modified Go/Nogo task, where the usual relation between stimulus and response (i.e., Go → respond; Nogo → refrain from responding) and an inverted version (i.e., Go → refrain from responding; Nogo → respond) was examined within each participant. The Go/Nogo task consisted of two different blocks. In the first block (compatible) one out of two words was presented on a PC monitor: 'DRÜCK' (German for 'PRESS'; Go stimulus) and 'STOP' (German for 'STOP'; Nogo stimulus) and the subjects were asked to respond within 500 ms on the 'DRÜCK' stimulus and refrain from responding on the 'STOP' stimulus. In trials with reaction times exceeding this deadline a feedback stimulus (1000 Hz, 60 dB SPL) was given 1200 ms after the response. This warning stimulus had to be avoided by the subjects. This time pressure was administered to strengthen response tendencies. The compatible block was always presented first, to generate a strong pre-potent response set and to strengthen usual stimulus–response mappings. In the second block subjects had to refrain from responding on the 'DRÜCK' stimulus and were requested to respond on the 'STOP' stimulus. In each block stimuli are displayed for 300 ms. The subjects had to react with the thumb to the Go stimuli and to refrain from responding to Nogo stimuli. The inter-trial interval (ITI) was jittered between 1600 and 1800 ms. 180 trials are presented in each block; 120 Go trials and 60 Nogo trials. This ITI length was also chosen to strengthen response tendencies.

2.3. EEG recording and analysis

EEG signals were recorded from 64 Ag-AgCl electrodes using standard positions according to the extended 10/20 system (Pivik et al., 1993) against a reference electrode located on Cz. The sampling rate of all recordings was 1 kHz, applying a filter bandwidth of 0.05–80 Hz to the EEG. Electrode impedances were kept below 5 kΩ. Horizontal and vertical eye-movements were corrected in the EEG using independent component analysis (ICA) (infomax algorithm) applied to the unsegmented data. Artifact rejection procedures were applied twice: automatically, with an amplitude threshold of ±80 μV, and visually by rejecting all trials contaminated by technical artifacts. Before quantifying ERPs the current source density (CSD) of the signals was calculated to achieve a reference-free evaluation (Nunez et al., 1997; Perrin, Pernier, Bertrand, & Echalier, 1989) using the following parameters: order of splines $m = 4$, and the maximum degree of the Legendre polynomials $n = 10$, with a precision of 2.72^{-7}. The exact mathematical procedure is explained in detail in Perrin et al. (1989).

Segmentation of the data was done twice: the first segmentation (for time domain analysis) was done segmenting epochs of 1200 ms length (−200 ms till presentation of the Go or Nogo stimulus at time point 0). Baseline correction was applied in the time interval between −200 ms and stimulus presentation. All subsequent peak quantification for standard ERP time-domain analysis was done relative to this baseline.

To achieve a reliable analysis of slow frequency components in subsequent time–frequency analyses the EEG was additionally segmented into 4096 ms long epochs with the Go or Nogo stimulus presentation being in the center of the analysis epoch (time point 0). The baseline was defined in the time window −800 till −600 ms before delivery of Go or Nogo stimulus, which is free of activity related to stimulus or response processing in the previous trial. These epochs and baseline were used for the time-frequency analysis (see details below). The number of trials included in the analyses was similar for both segmentations ($p > .5$).

Table 1
Demographical data of the pre-manifest HD gene mutation carriers group and the healthy control group. The mean and standard deviation (SD) are given.

Parameter	pre-HD	Control
N	25	25
Age	39.36 (10.04)	39.12 (9.5)
Sex	14 female/11 male	14 female/11 male
CAG	42.08 (1.78)	NA
Disease burden score (DBS)	253.5 (75.25)	NA
Years to onset (YTO)	15.66 (8.3) median = 13.75	NA
5-Year probability	17.42 (17.51) median = 12.05	NA
UHDRS motor score (MS)	2.80 (2.78)	NA
UHDRS total functional capacity scale (TFC)	12.96 (0.2)	NA
UHDRS Instrumental Scale (IS)	99.4 (1.6)	NA
UHDRS Cognitive Score (CS)	329.40 (43.35)	NA

On trials denoting response inhibition the Nogo-N2 was defined as the most negative deflection within the range of 150–300 ms after stimulus onset. The Nogo-P3 was defined as the most positive deflection from 320 till 500 ms. Amplitudes of the Go-N2 and Go-P3 were measured at the corresponding time point, where the Nogo component reached its maximum (Beste, Willemssen, et al., 2010; Beste, Dziobek, et al., 2009). The N2 was measured at electrode Fz, FCz and Cz. For the P3 electrode FCz was used. However, to underline that the Nogo-P3 is different from the usual P3b, also electrode Pz was included in analysis.

2.4. Time–frequency analysis and calculation of the phase-locking factor (PLF)

Time–frequency (TF) analysis of stimulus-related potentials was performed by means of a continuous wavelet transform (CWT) applying Morlet wavelets. Complex Morlet wavelets w can be generated in the time domain for different frequencies, f, according to the equation:

$$w(t,f) = A \exp\left(\frac{-t^2}{2\sigma_t^2}\right) \exp(2i\pi ft),$$

where t is time, $A = (\sigma_t\sqrt{\pi})^{-1/2}$, σ_t is the wavelet duration, and $i = \sqrt{-1}$. For analysis and TF-plots, a ratio of $f_0/\sigma_f = 5.5$ was used, where f_0 is the central frequency and σ_f is the width of the Gaussian shape in the frequency domain. The analysis was performed in the frequency range 0.1–20 Hz with a central frequency at 0.5 Hz intervals. For different f_0, time and frequency resolutions can be calculated as $2\sigma_t$ and $2\sigma_f$, respectively. σ_t and σ_f are related by the equation $\sigma_t = 1/(2\pi\sigma_f)$. For example, for $f_0 = 3$ Hz, $2\sigma_t = 425$ ms and $2\sigma_f = 1.5$ Hz; for $f_0 = 5$ Hz, $2\sigma_t = 255$ ms and $2\sigma_f = 2.5$ Hz. For each trial, the time-varying power in a given frequency band was calculated, which was obtained by squaring the absolute value of the convolution of the signal with the complex wavelet. Frequency-relevant TF powers were extracted in the central frequency of the delta ($f_0 = 3$ Hz) and theta frequency band ($f_0 = 6$ Hz), as well as in the lower alpha frequency band ($f_0 = 10$ Hz) (see: Ocklenburg, Güntürkün, & Beste, 2011).

Maximal TF power and corresponding peak power latencies were measured in the time intervals used for ERP quantification. A time window of 600–800 ms prior to the response was used to estimate background noise and wavelet power in the time range of interest was measured normalized to wavelet power at this baseline. As the ITI is jittered between 1600 and 1800 ms this baseline, relative to the begin of stimulus presentation (i.e., a new trial), is free of the before trial activity. TF power was log 10-transformed to normalize the distributions for statistical analyses.

In the current study, the total power of the ERP-signal was analyzed. Analysis was restricted to the total power of the signal, because this measure is used to calculate the phase-locking factor, giving a measure of the reliability of neural synchronization processes in time and frequency across trials (PLF; Roach & Mathalon, 2008; Tallon-Baudry et al., 2001). The PLF is independent of the signal's amplitude (Kolev & Yordanova, 1997). The values of PLF vary between 0 and 1, with values of 1 indicating perfect phase-locking or phase alignment across trials, whereas values close to 0 reflect high phase variability. The whole analysis procedure is comparable to Beste, Kolev, et al. (2010).

2.5. Statistical analysis

Kolmogorov–Smirnov tests revealed that all relevant variables were normally distributed (all $z < 0.5$; $p > .4$; one-tailed). Data was analyzed using repeated and univariate analyses of variance (ANOVAs). In the repeated measures ANOVAs, the factors "electrode", "trial type (Go vs. Nogo)" and "context (compatible vs. incompatible)" were used as within-subject factors. The factor "group" (pre-HD vs. controls)" was used as between-subject factor. When appropriate, the degrees of freedom were adjusted using Greenhouse–Geisser correction. Post hoc tests performed were adjusted using Bonferroni correction, when necessary. In Section 3 always the most complex interaction between the different factors is described. As a measure of variability the standard error of the mean (SEM) is given. These latter analyses were restricted to behavioural and neurophysiological parameters that showed largest differences between pre-HDs and controls in the initial ANOVAs.

3. Results

In the following, the results of the behavioural and neurophysiological data analyses are presented. The results are presented as follows: Trials presenting ‚PRESS' in the compatible condition and ‚STOPP' in the incompatible condition are referred to as ‚Go-trials'; trials presenting ‚STOPP' in the compatible condition and 'PRESS' in the incompatible condition are referred to as 'Nogo-trials'.

3.1. Behavioural data

For the behavioural data, the absolute frequency of correctly executed and correctly inhibited responses for the pre-HD and control group is given in Fig. 1.

The ANOVA revealed an interaction "Go/Nogo × condition × group" ($F(1,48) = 5.63$; $p = .022$, $\eta^2 = .11$). Subsequent post hoc tests revealed that within the pre-HD and control group, accuracy was better upon Go-trials than upon Nogo-trials presentation in the compatible and the incompatible condition (all $t(24) > 10.1$; $p < .001$) (refer Fig. 1). Between-condition comparisons revealed that performance on incompatible Nogo trials was dysfunctional in pre-HDs ($t(24) = 28.45$; $p < .001$) and controls ($t(24) = 10.88$; $p < .001$), when compared with the compatible condition. The difference in Nogo trial performance between the compatible

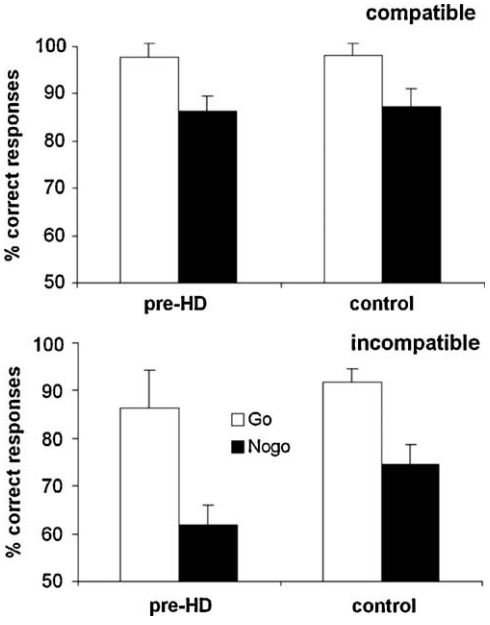

Fig. 1. Mean absolute frequency of correct responses in the compatible (top) and incompatible (bottom) block, separated for the control and pre-HD group. White bars represent performance on Go-trials, black bars denote performance on Nogo-trials. Error bars denote standard error of the mean (SEM).

and the incompatible condition was larger in the pre-HD group ($t(24) = 28.45$; $p < .001$) than the control group ($t(24) = 10.88$; $p < .001$). This is underlined, when using this difference score in an independent sample t-test showing that performance decline was stronger in pre-HDs than in controls ($t(48) = -9.24$; $p < .001$). On Go trials declines in performance for the incompatible condition were evident in pre-HDs ($t(24) = 5.47$; $p < .001$) and controls ($t(24) = 8.43$; $p < .001$). Yet, when calculating this difference in performance between compatible and incompatible trials in pre-HDs and controls, t-tests revealed that there was no difference in performance decline between pre-HDs and controls ($t(48) = 1.85$; $p > .1$).

Within the pre-HD group, there were no differences between subjects close and far to EAO on Go and Nogo trial performance, as indicated by a repeated measures ANOVA using cEAO and fEAO as between subject factor and Go and Nogo-trials in the incompatible condition as within subject factor (all $F < 0.9$; $p > .2$). Similarly, also the dichtomization in high and low 5-year onset probability (hprob and lprob) did not reveal effects (all $F < 0.5$; $p > .3$). Reaction times (RTs) did not differ between the conditions (all $F < 0.9$; $p > .3$) and there were also no other significant main or interaction effects (all $F < 0.7$; $p > .4$).

To analyze behavioural parameters with respect to possible changes in performance throughout the incompatible block, this block was bisected into two halves. Comparing behavioural performance between the halves did not reveal any main effect "halves", or an interaction with the factor group (all $F < 0.4$; $p > .6$).

3.2. Neurophysiological data: time domain analysis

Stimulus-locked potentials for Go and Nogo trials in the compatible and incompatible conditions are shown in Fig. 2A for pre-HDs and controls separately.

N2 effects: The repeated measures ANOVA revealed an interaction "electrode × Go/Nogo × condition × group" ($F(1,48) = 9.23$; $p < .005$; $\eta^2 = .19$). Subsequent ANOVAs revealed that an interaction "Go/Nogo × condition × group" ($F(1,48) = 14.73$; $p < .001$; $\eta^2 = .24$) was only evident for electrode FCz, but not for the other electrodes (F's < 1.1; $p > .3$). Therefore only electrode FCz was analyzed further. In compatible Go and Nogo-trials, pre-HDs and controls did not differ in their N2 amplitudes (Go: $t(48) = -0.52$; $p = .5$; Nogo: $t(48) = -0.5$; $p = .6$) (refer Fig. 2A). Within each group the N2 on Nogo-trials was always larger in the compatible condition (all $t(24) > 11.7$; $p < .001$) (refer Fig. 2A).

In the incompatible condition, pre-HDs revealed an attenuated N2 on Nogo-trials, compared to controls (pre-HDs: -8.8 ± 0.7; controls: -14.5 ± 0.6) ($t(48) = 6.77$; $p < .001$) (refer Fig. 2A). No group differences were evident for Go-trials in this condition ($t(48) = -1.3$; $p = .16$). Compared to the compatible condition, the Nogo-N2 was attenuated in pre-HDs and controls in the incompatible condition ($t(24) > 4$; $p < .001$). The degree of attenuation (calculated as the difference between compatible minus incompatible) was larger in pre-HDs (9.3 ± 0.6), than in controls (4.5 ± 0.4) ($t(48) = 5.11$; $p < .001$). There were generally no latency effects in the N2 data (all $F < 0.8$; $p > .3$). There were no differences between subjects close and far from EAO (all $F < 0.7$; $p > .3$), and when using the dichotomization of the 5-year onset probabilities (all $F < 0.6$; $p > .3$).

P3-effects: There was an interaction "electrode × Go/Nogo × compatibility × group" ($F(1,48) = 8.21$; $p = .006$; $\eta^2 = .14$). Exploring this interaction further, an interaction "Go/Nogo × compatibility × group" was only evident for electrode FCz ($F(1,48) = 15.92$; $p < .001$; $\eta^2 = .24$), but not for electrode Pz ($F(1,48) = 0.11$; $p > .7$; $\eta^2 = .002$). Therefore, only electrode FCz was analyzed further. Independent sample t-tests revealed that both groups did not differ in amplitudes upon Go-trials in the compatible ($t(48) = .18$; $p > .8$), and incompatible condition ($t(48) = .55$; $p > .5$) (refer Fig. 2). Upon Nogo-trials, the pre-HD group revealed lower amplitudes than controls in both conditions (compatible: $t(48) = -4.23$; $p < .001$: incompatible: $t(48) = -4.11$; $p < .001$) (refer Fig. 2A). There were generally no latency effects in the P3 data (all F's < 0.7; $p > .4$).

In summary, the Nogo-P3 was attenuated in the pre-HD group, compared to the control group. This attenuation did not differ between task conditions. Opposed to that, an attenuation of the Nogo-N2 in the pre-HD group was only evident in the incompatible task condition and parallels the behavioural results pattern.

N1 effects: To ensure that the effects observed in the behavioural data and ERPs reflecting response inhibition processes (Nogo-N2, Nogo-P3) are not biased with respect to different visual attentional processes in pre-HDs and controls, we examined the modulation of the N1 between both groups in the different experimental conditions (compatible vs. incompatible) on Go and Nogo-trial presentation. The N1 is a reliable marker of visual attentional processing reflecting modulations of the magnitude of neural responses to incoming stimuli (e.g. Mangun, 1995). The N1 is depicted in Fig. 2B. The N1 was measured at electrodes PO7 and PO8, which revealed the maximum potentials as suggested by scalp topography maps. The repeated measures ANOVA only revealed that the N1 was larger at electrode PO7, compared to PO8 ($F(1,48) = 9.1$; $p < .001$). All other main and interaction effects with "group" were not significant (all $F < 0.5$; $p > .5$), suggesting that attentional processes are not different between the groups and hence do not modulate response inhibition processes. As with the behavioural data, neither of the above ERP-parameters differed, when comparing the first and second half of the incompatible block. There was also no interaction with "group" (all $F < 0.4$; $p > .6$).

3.3. Neurophysiological data: time–frequency analysis

Time–frequency decomposition was performed for ERPs reflecting response inhibition processes and were restricted to electrode FCz, since this electrode reflected effects in the time-domain analysis, as described above. The effects in this analysis parallel the results of the time-domain analysis.

N2 total power: The repeated measures ANOVA revealed a significant interaction "frequency band × Go/Nogo × compatibility × group" ($F(2,96) = 4.18$; $p < .05$; $\eta^2 = .1$). Subsequent ANOVAs revealed that only in the delta frequency band an interaction "Go/Nogo × compatibility × group" was evident ($F(1,48) = 4.94$; $p = .01$; $\eta^2 = .1$). Bonferroni-corrected post hoc tests revealed that in the compatible block total delta band power was generally higher in Nogo trials (controls: 5.34 ± 0.2; pre-HD: 5.39 ± 0.3) than in Go trials (controls: 2.88 ± 0.3; pre-HD: 2.77 ± 0.3) (all $t(24) > 4.9$; $p < .001$) with no difference between groups ($t(24) = 0.3$; $p > .3$). In the incompatible condition, Nogo-N2 total wavelet power was weaker in pre-HDs (2.9 ± 0.2) compared to controls (3.77 ± 0.1) ($t(48) = 2.99$; $p < .01$). Compared to the compatible condition, the Nogo-N2 total wavelet power was attenuated in pre-HDs and controls ($t(24) > 4$; $p < .001$). Yet, the degree of attenuation in Nogo trials (calculated as the difference between compatible minus incompatible) was larger in pre-HDs (2.49 ± 0.3), than in controls (1.57 ± 0.2) ($t(48) = 3.01$; $p < .01$). No difference in total delta band power was evident between Go (2.85 ± 0.3) and Nogo-trials (2.9 ± 0.2) with the pre-HD group ($t(24) = 0.3$; $p > .2$), while in controls the delta power was higher on Nogo (3.77 ± 0.1), than Go-trials (2.83 ± 0.3) ($t(24) = 6.3$; $p < .001$). There were no differences between subjects close and far to EAO (all F's < 0.7; $p > .4$), and also no differences between subjects with high or low 5-year onset probability. The N2 total power data, therefore completely parallels the N2-data in the time-domain analysis.

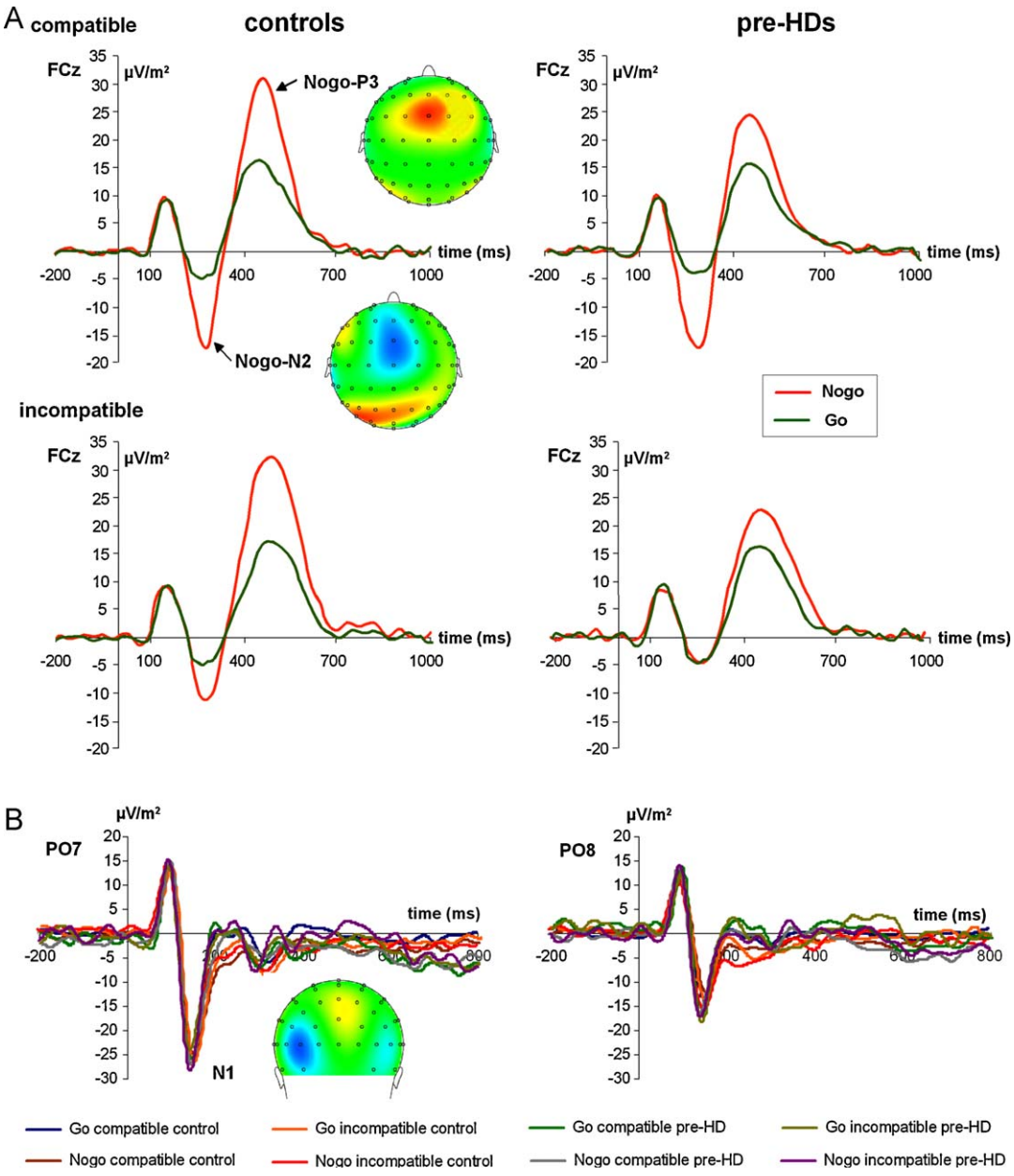

Fig. 2. (A) Stimulus-locked event-related potentials (ERPs) depicted at electrode FCz, separated for the compatible and incompatible condition as well as for controls and pre-HDs. Time point 0 denotes the time point of stimulus delivery. Red lines denote the potential upon Nogo-trials, green lines denote the potential upon Go-trials presentation. The scalp topographies denote the Nogo-N2 and Nogo-P3 component. (B) Stimulus-locked ERPs at electrode PO7 and PO8 depicting the N1 event-related potential. The different colours denote the varying conditions in controls and pre-HDs. The N1 scalp topography is given.

P3 total power: Similar to the N2 total power, there was an interaction "frequency band × Go/Nogo × compatibility × group" ($F(2,96) = 5.22$; $p < .05$; $\eta^2 = .13$) and again the interaction "Go/Nogo × compatibility × group" was only evident in the delta frequency band ($F(1,48) = 5.66$; $p < .01$; $\eta^2 = .14$). In the compatible condition, total delta band power was higher in Nogo trials (controls: 9.68 ± 0.3; pre-HD: 7.41 ± 0.3), than in Go trials (control: 5.44 ± 0.4; pre-HD: 5.37 ± 0.3) ($t(24) = 6.3$; $p < .001$) with pre-HDs showing lower delta power than controls upon Nogo-stimuli ($t = 4.1$; df = 48; $p < .001$). For the incompatible block, power was higher on Nogo-trials (controls: 8.34 ± 0.4; pre-HD: 6.99 ± 0.2), than on Go-trials (control: 5.36 ± 0.3; pre-HD: 5.4 ± 0.3) in controls ($t(24) = 2.66$; $p = .01$) and pre-HDs ($t(24) = 1.7$; $p < .05$). Pre-HDs also revealed lower power upon Nogo-trials than controls ($t(48) = 2.11$; $p < .05$). There were no differences between subjects close and far to EAO (all $F < 0.3$; $p > .5$) and with high or low 5-year onset probability (all $F < 0.3$; $p > .5$). In summary, the results of P3 total power wavelet analysis parallel the results of the time-domain analysis. Similar to the time-domain analysis, no main or interaction effects were observed comparing the two halves (all $F < 0.8$; $p > .3$).

3.4. Neurophysiological data: phase-locking analysis

The phase-locking factors (PLFs) for each condition (Go vs. Nogo and compatible vs. incompatible) are depicted in Fig. 3 for the pre-HD and control group for electrode FCz. The PLF was quantified around the respective peak in the time-domain analysis (ERPs).

N2-PLF: The repeated measures ANOVAs across the phase-locking factors (PLFs) in the N2 range revealed a significant interaction "frequency band × Go/Nogo × compatibility × group" ($F(2,96) = 9.14$; $p < .001$; $\eta^2 = .17$). Only for the delta frequency band, an interaction "Go/Nogo × compatibility × group" was

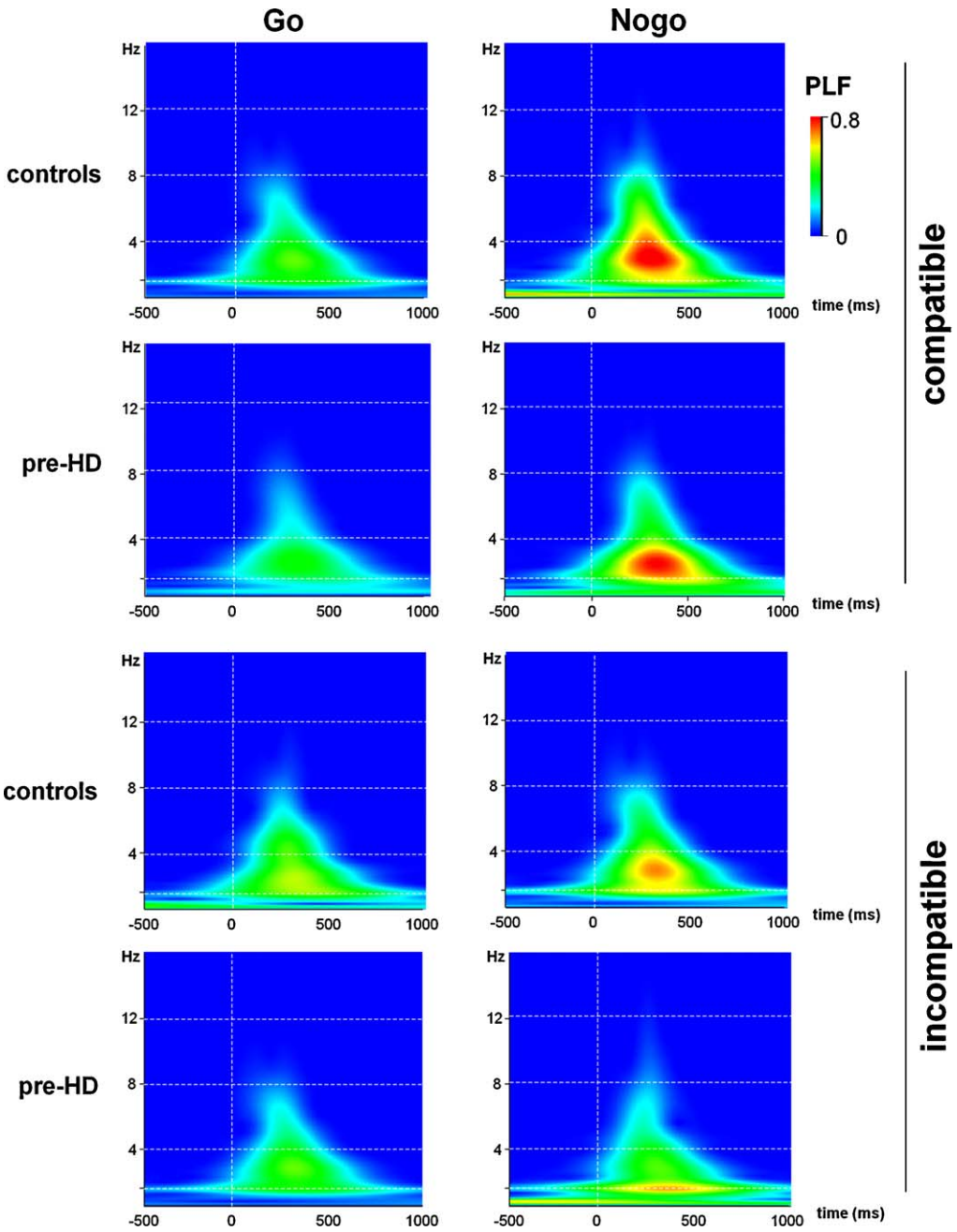

Fig. 3. Plots of the phase-locking factor (PLF) at electrode FCz, separated for the control and pre-HD group, compatible and incompatible condition and Go and Nogo-trials. The degree of phase-locking is colour-coded. The ordinate denote the frequency (in Hz), the abscissa denotes the time (in ms). White dashed lines denote the frequency band boundaries related to the delta (1.5–3.5 Hz), theta (4–8 Hz) and alpha frequency band (8–12 Hz). The time point 0 denotes the time point of stimulus delivery.

evident ($F(1,48) = 7.94$; $p = .007$; $\eta^2 = .14$). Hence, only the delta frequency band was analyzed further.

Bonferroni-corrected post hoc tests revealed that the PLF was higher for Nogo than for Go-trials in the compatible condition in pre-HDs and controls (all $t(24) > -7.24$; $p < .001$) and also the groups did not differ from each other in the PLF on Go and Nogo trials ($t < 1.1$; $p > .9$). For the incompatible condition, the between group effect in PLF was larger for Nogo ($t(48) = -11.63$; $p < .001$), than for Go trials ($t(48) = -5{,}83$; $p < .001$). Furthermore, the reduction of PLF on compatible compared to incompatible Nogo trials was stronger in pre-HDs (0.24 ± 0.02), than in controls (0.05 ± 0.01) ($t(48) = 8.01$; $p < .001$).

Similar to the N2 amplitude and total wavelet power data, there were no differences between subjects close and far to EAO (all $F < 1.1$; $p > .2$) and with high or low 5-year onset probability (all $F < 0.9$; $p > .2$). Contrary to pre-HDs, PLFs were higher upon Nogo-trials, compared to Go-trials in the control group in the incompatible condition ($t(24) = 6.75$; 24; $p < .001$) (refer Fig. 3). In the delta frequency band PLFs were generally lower in pre-HDs, compared to controls (main effect group: $F(1,48) = 52.37$; $p < .001$; $\eta^2 = .52$). Also, PLFs were generally lower for the incompatible compared to the compatible condition (main effect condition: $F(1,48) = 106.68$; $p < .001$; $\eta^2 = .69$).

P3-PLF: Analyzing phase-locking in the P3 range (i.e., from 320 to 500 ms) using the above ANOVAs did not reveal any significant effects (all $F < 0.7$; $p > .3$).

As with the total power analyses, no main or interaction effects were observed, when comparing the two halves of the incompatible

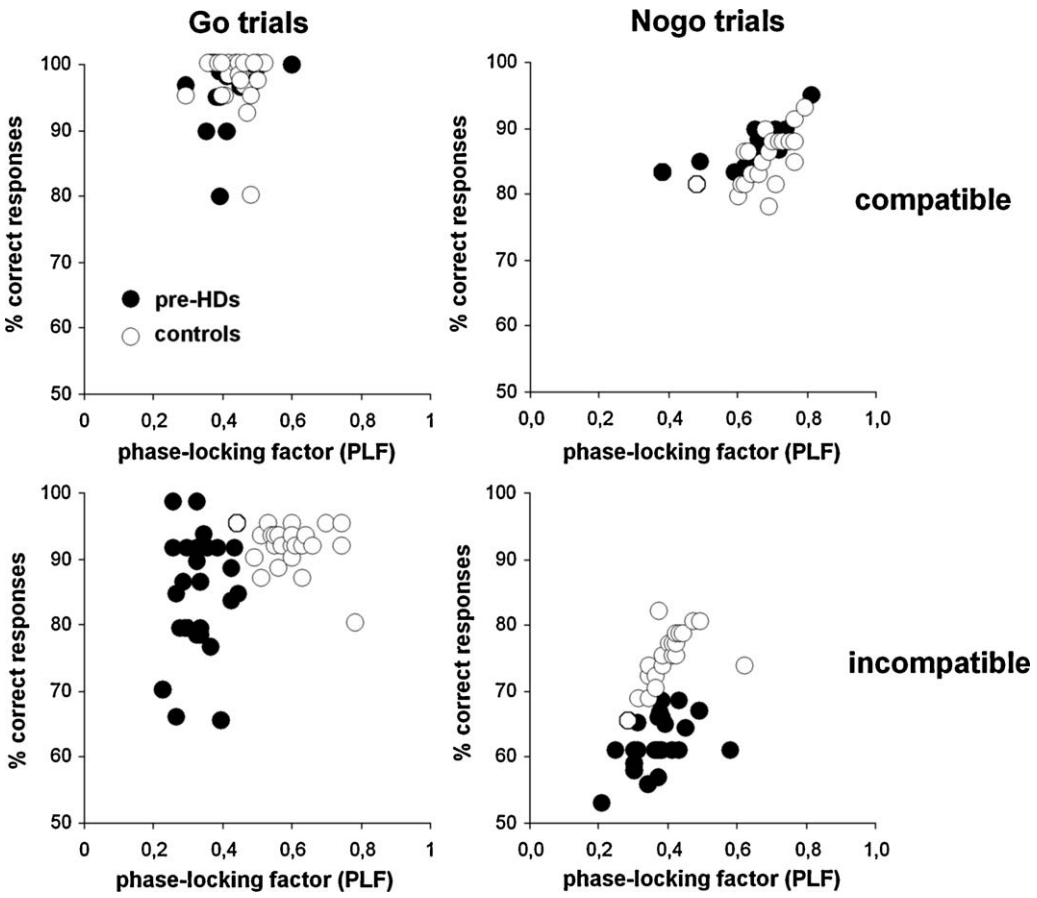

Fig. 4. Correlation between the degree of phase-locking and behavioural performance upon Go (left) and Nogo-trials (right) for the compatible (top) and incompatible condition (bottom). White circles denote pre-HD subjects, black circles denote control subjects.

block (all $F < 0.7$; $p > .4$). In summary, the phase-locking data parallel the pattern observed in the time domain and total wavelet power analysis.

3.5. Regression analyses

Regression analyses were performed to examine the interrelation of N2 phase-locking processes and behavioural performance. To this end, linear regression models were calculated using phase-locking in the delta frequency band and group as regressors to predict behavioural performance. As can be seen in Fig. 4, higher degrees of phase-locking were related to better behavioural performance (more correct rejections) on Nogo trials in the compatible condition ($\beta_{PL}F = .674$; $t = 6.17$; $p < .001$), not differing between groups ($\beta_{group} = -.001$; $t = -0.01$; $p > .9$) ($F(2,47) = 19.55$; $p < .001$).

However, group differences were evident when applying the same model to predict behavioural performance in incompatible Nogo-trials ($\beta_{group} = .344$; $t = 2.28$; $p < .001$) ($F(2,47) = 157.02$; $p < .001$). Fig. 4 shows that higher degrees in phase-locking were related to better behavioural performance in controls ($r = .581$; $R^2 = .26$; $p = .007$), but no correlation was evident in pre-HDs in the incompatible condition ($r = .06$; $R^2 = .1$; $p > .3$). The lack of relation between the degree of phase-locking and behavioural performance seems therefore to be specific for the incompatible condition. Using total wavelet power as regressor instead of delta PLF, did not reveal any significant regression model (all $F < 0.6$; $p > .3$). Also, when correlating the individual decline in phase-locking (i.e., $PLF_{Nogo\text{-}compatible} - PLF_{Nogo\ incompatible}$) with the individual declines in behavioural performance across conditions (i.e., $Nogo_{compatible} - Nogo_{incompatible}$) there was a correlation in the healthy control group suggesting that a larger difference in phase-locking was related to a larger difference in behavioural performance between groups ($r = .44$; $R^2 = .17$; $p = .012$). In the pre-HD group no correlation was evident ($r = .18$; $R^2 = .2$; $p > .2$), suggesting for a phase-locking-behavioural decoupling in pre-HDs.

Additional regression analyses were performed to examine how far the observed declines in phase-locking (i.e., $PLF_{Nogo\text{-}compatible} - PLF_{Nogo\ incompatible}$) are related to the individual's disease status. To this end, we calculated the 5-year onset probability for each pre-HD subject according to the prediction model by Langbehn et al. (2004). The results of the regression analysis are given in Fig. 5.

Fig. 5A suggests an exponential decline of phase-locking between the experimental conditions with increasing probability to enter the symptomatic disease stage in the next five years. An exponential regression function revealed a 13% higher amount of explained variance ($F(1,23) = 34.56$; $p < .001$; $r = .79$; $R^2 = .62$) than a linear regression model ($F(1,23) = 22.59$; $p < .001$; $r = .66$; $R^2 = .43$). When using "years-to-onset (YTO)" (Langbehn et al., 2004) as predictor the decline in phase-locking in the incompatible compared to the compatible condition was higher with fewer YTO. Both, an exponential ($F(1,23) = 37.72$; $p < .001$; $r = .80$; $R^2 = .64$) and a linear regression function ($F(1,23) = 41.43$; $p < .001$; $r = 0.79$; $R^2 = .62$) explained a comparable amount of variance with a difference of only 2% between the models (refer Fig. 5B). There was also a substantial correlation between the 'disease burden score (DBS)' and the degree decline in phase-locking ($r = .764$; $R^2 = .57$; $p < .001$), suggesting that gene mutation carriers with a higher DBS also revealed stronger decline in phase-locking (refer Fig. 5C).

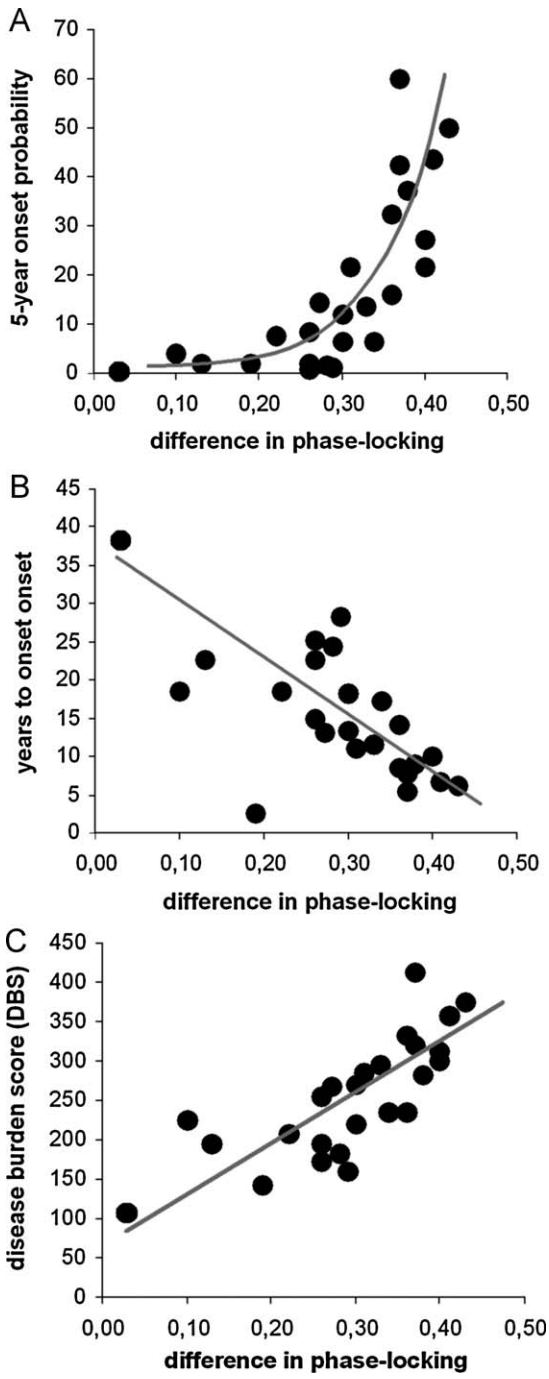

Fig. 5. Correlation of the difference in phase-locking between the compatible and incompatible conditions in trials requiring the inhibition of responses in pre-HD subjects. The difference in phase-locking is calculated as $PLF_{Nogo\text{-}compatible} - PLF_{Nogo\ incompatible}$ and reflects the degree as to which phase-locking declines by increasing difficulty of stimulus–response mapping in the incompatible task. Part (A) denotes a exponential relation of this difference in phase-locking with the probability to enter manifest disease stage in the next five years. Part (B) denotes a linear relation with the years until the estimated age of onset. Part (C) denotes the correlation of the 'disease burden score (DBS)' with the decline in phase-locking in pre-manifest gene mutation carriers.

4. Discussion

We examined pre-manifest HD gene mutation carrier's ability to integrate sensory inputs with contextual information to drive response inhibition processes. This was done to examine, how far changes in the precision of neural synchronization processes are induced by only slight dysfunctions of striatal neural interconnectivity and in how far such slight changes may affect action selection processes.

Pre-manifest HD gene mutation carriers (pre-HDs) revealed substantial response inhibition deficits, when changes in contextual information alter mappings of a visual stimulus to the appropriate response and interferes with an existing and previously strengthened stimulus–response mapping. Group differences, depending on compatible vs. incompatible Go/Nogo task condition, were evident on Nogo trials but not on Go trials. Therefore, especially response inhibition opposed to the execution of responses was differentially affected by variations in the experimental conditions. An in-depth neurophysiological analysis revealed that response inhibition deficits in pre-HDs observed at the behavioural level were mediated by specific alteration in response inhibition subprocesses: the N2 ERP amplitude and total wavelet power was attenuated and also the related phase-locking factor (PLF), reflecting the reliability of neural synchronization processes in time and frequency was weaker. The degree in phase-locking was related to task performance and depended on the amount of the individual's mutant huntingtin exposure ('disease burden score'; Penney et al., 1997; Tabrizi et al., 2009) as well as the probability to enter the symptomatic stage within a certain time period (Langbehn et al., 2004). The changes observed cannot be due to known deficits in task switching in pre-HD (Aron et al., 2003), since response inhibition deficits in pre-HDs were seen throughout the incompatible block with no effects of "time-on task". Also known dysfunctions in attentional processes (e.g. Stout et al., 2011) may be less relevant, since no effects in the N1 were observed.

In the compatible condition, the N2 was larger (i.e., more negative) on Nogo, compared to Go-trials in controls and pre-HDs. Both groups did not differ in their Go and Nogo-N2 amplitudes and revealed a similar high level of response inhibition performance that was closely related to the degree of phase-locking in the N2-range. These results suggest that pre-motor inhibition or conflict processing, as reflected by the Nogo-N2 (Beste, Dziobek, et al., 2009; Falkenstein, Hoormann, & Hohnsbein, 1999; Nieuwenhuis et al., 2003) are similarly efficient in pre-HDs and controls in the compatible condition. According to the pre-motor inhibition hypothesis of the Nogo-N2 (Falkenstein et al., 1999) a more negative Nogo-N2 suggests an increase in pre-motor inhibition reducing the tendency to respond on Nogo-trials (Falkenstein et al., 1999). The finding that a higher reliability of neural synchronization in time and frequency (i.e., high PLF) in the Nogo-N2 time range is related to better behavioural performance (i.e., fewer false alarms) fits well to the pre-motor inhibition hypothesis, stating that the Nogo-N2 reflects the inhibition of a mistakenly selected motor program (Beste, Dziobek, et al., 2009; Beste et al., 2008a; Falkenstein et al., 1999). The pattern of results in the compatible condition replicates the pattern found in a previous study (Beste, Willemssen, et al., 2010). Also in line with this previous study (Beste, Willemssen, et al., 2010) the Nogo-P3 was attenuated in pre-HDs, compared to controls in the compatible condition and also total wavelet power was attenuated in pre-HDs. The degree of phase-locking was not different between the groups and did not affect behavioural performance as indicated by regression analyses. The Nogo-P3 effects have to be treated cautiously, as oddball-effects that may emerge due to the lower frequency of Nogo, compared to Go trials cannot be ruled out to modulate the P3 effects.

In the incompatible condition, the pattern of results changed: In pre-HDs, the Nogo-N2 amplitude was attenuated relative to the compatible condition and also compared to controls in the incompatible condition. The Nogo-N2 attenuation, relative to the compatible condition, was stronger in pre-HDs than in controls. In both groups, this was paralleled by decreases in the rate of correct

rejections, which was also higher in pre-HDs. As the Nogo-N2 attenuation and the attenuation of Nogo-N2-PLF was stronger in pre-HDs than in controls, pre-motor inhibition processes (Falkenstein et al., 1999) appear to be more compromised in pre-HDs than in controls, when discordant contextual and sensory information has to be integrated. The phase-locking factor (PLF) analyses further revealed that performance in pre-HDs was also not related to the PLF, which is in contrast to the compatible condition. In controls, behavioural performance was still related to the degree of phase-locking. This decoupling of behavioural performance from phase-locking in pre-HDs likely reflects the dysfunctional integration of sensory and contextual inputs in the incompatible condition in pre-HDs.

Neural synchronization processes depend on the interconnectivity between neural assemblies (Kitano & Fukai, 2004; Lago-Fernandez et al., 2001). The observed decrease in the reliability of neural synchronization in time and frequency with subsequent dysfunctions in response inhibition processes most likely emerge due to already evident neurodegenerative changes in pre-manifest HD compromising neural inter-connectivity (e.g. Cepeda et al., 2007; Rosas et al., 2008; Tabrizi et al., 2009). In a recent study by our group we argued that processes reflected by the N2 in response inhibition may depend on the nigro-striatal system modulating MSNs (Beste, Willemssen, et al., 2010). As MSNs are important for the integration of various streams of information (e.g. Bar-Gad et al., 2003; Gurney et al., 2004; Redgrave & Gurney, 2006; Redgrave, Prescott, & Gurney, 1999) and are early affected in HD (Cepeda et al., 2007; Mitchell et al., 1999) it is possible that the cognitive deficit observed may be due to MSN neuron degeneration and weakening of MSN interconnectivity. The lack of group differences in neurophysiological processes related to attentional selection (i.e., N1) also suggest that deficits observed emerge at a point in processing where contextual information and visual input are integrated and not already at attentional selection stages. In HD, MSNs reveal an increased vulnerability to mutant huntingtin, which is higher than vulnerability of cortical neurons (e.g. Thomas et al., 2011). Our correlational results show that subjects with a higher lifetime exposure to mutant huntingtin (disease burden score) (Penney et al., 1997; Tabrizi et al., 2009) revealed stronger declines in phase-locking than pre-HD with lower disease burden. Since mutant huntingtin especially compromises striatal MSN functioning (e.g. Thomas et al., 2011), this result underlines that the mechanisms leading to the observed effects may be due to MSN dysfunction. The fact that response inhibition in the compatible condition was not affected suggests that MSN dysfunctions only become critical, when action selection processes become more demanding. More habitual stimulus–response mappings (compatible condition) seem to be resolved even in compromised MSN networks.

Because of a strong interrelation of the CAG-repeat length related disease burden score with measures giving an estimate of disease manifestation in the next years (i.e., a higher probability of disease manifestation in the next five years and fewer 'years to onset (YTO)' (Langbehn et al., 2004)), these were also related to declines in phase-locking. Interestingly, in pre-HD subjects with lower probability to enter the manifest stage in the next five years, the slope of the regression curve was flatter than in subjects with higher onset probability in the next five years. This suggests that declines in the reliability of neural synchronization in time and frequency may be particularly sensitive to changes in pre-HD subjects with a higher probability to enter the manifest stage within in the next five years. The fact that no differences between pre-HD subjects dichotomized in "close to EAO" and "far to EAO" as well as "high (hprob)" and "low 5-year onset probability (lprob)" subgroups were evident, suggests a higher sensitivity of continuous CAG-age measures over dichotomized measures to identify possibly sensitive pre-manifest disease progression markers (see also: Langbehn et al., 2004).

The current study adds to growing evidence that electrophysiological techniques may serve as biomarkers in HD (for review: Nguyen, Bradshaw, Stout, Croft, & Georgiou-Karistianis, 2010). In this respect several studies accounted for robust declines in various ERPs reflecting different cognitive processes (e.g. Antal et al., 2003; Beste, Saft, Andrich, Gold, & Falkenstein, 2008b; Beste, Willemssen, Saft, & Falkenstein, 2009; Münte et al., 1997). Yet, only a few studies accounted for alterations in the pre-manifest stage (for review: Nguyen et al., 2010). In this stage, the neurophysiological pattern of modulation is less clear: some processes seem to be already dysfunctional (e.g. Beste et al., 2008b; van der Hiele et al., 2007), while other results point towards intensified neurophysiological processes that may reflect compensatory efforts (Beste et al., 2007) or a gain of functioning that leads to superior cognitive performance in some domains in the manifest stage (Beste, Saft, Güntürkün, & Falkenstein, 2008). In contrast to the study by Beste et al. (2007) examining error monitoring processes the current results do not suggest for compensatory processes in pre-HD. However, response inhibition and error monitoring processes are most likely mediated via different basal ganglia-prefrontal loops (e.g. Beste, Baune, Domschke, Falkenstein, & Konrad, 2010b) and may therefore be differentially modulated in pre-HDs. A more detailed analysis of such a possible differential modulation of different fronto-striatal loops in pre-manifest HD may prove useful to understand processes occurring in pre-manifest HD and may be valuable to track pre-manifest disease progression in future longitudinal studies.

In summary, the behavioural results show that pre-HD subjects encounter problems when discordant contextual information and sensory input have to be integrated to enable response inhibition. No deficits were evident, when response inhibition can be based on more habitual stimulus–response mappings, i.e., when contextual and sensory information were congruent. The results suggest that pre-HD's fronto-striatal loops become overstrained by increasing the complexity of action selection. While 'habitual' action selection is unaffected by changes in striatal structures influencing reliability of neural synchronization processes, efficient 'controlled' processes of action seem to be closely dependent upon highly reliable neural synchronization processes. The neurophysiological analysis suggests that especially pre-motor inhibition processes (Nogo-N2) are affected. This was most strongly reflected in a decline in the degree of phase-locking in the Nogo-N2 range. Deficits in pre-HDs seem to emerge as a consequence of phase-locking-behavioural decoupling. Of clinical interest, declines in the precision of phase-locking depended on the amount of the individual's mutant huntingtin exposure and predicted the probability of disease manifestation in the next five years. This suggests that phase-locking parameters may prove useful in future studies evaluating a possible function as a biomarker in Huntington's disease.

Acknowledgements

The research was supported by a FoRUM grant, University of Bochum (AZ: K040-2009) to C.S. and partly by a Grant from the CHDI foundation and by to C.B. and C.S. We thank all participants.

References

Antal, A., Beniczky, S., Kincses, T. Z., Jakab, K., Benedek, G., & Vecsei, L. (2003). Perceptual categorization is impaired in Huntington's disease: An electrophysiological study. *Dementia Geriatric Cognitive Disorders*, *16*, 187–192.

Aron, A. R., Watkins, L., Sahakian, B. J., Monsell, S., Barker, R. A., & Robbins, T. W. (2003). Task-set switching deficits in early stage Huntington's disease: Implications for basal ganglia function. *Journal of Cognitive Neuroscience*, *15*, 629–642.

Band, G. P., & van Boxtel, G. J. (1999). Inhibitory motor control in stop paradigms: review and reinterpretation of neural mechanisms. *Acta Psychologica (Amst.)*, *101*, 179–211.
Bar-Gad, I., Morris, G., & Bergman, H. (2003). Information processing, dimensionality reduction and reinforcement learning in the basal ganglia. *Progress in Neurobiology*, *71*, 439–473.
Beste, C., Baune, B. T., Domschke, K., Falkenstein, M., & Konrad, C. (2010a). Paradoxical association of the brain-derived-neurotrophic factor Val66Met genotype with response inhibition. *Neuroscience*, *166*, 178–184.
Beste, C., Baune, B. T., Domschke, K., Falkenstein, M., & Konrad, C. (2010b). Dissociable influences of NR2B-receptor related neural transmission on functions of distinct associative basal ganglia circuits. *Neuroimage*, *52*, 309–315.
Beste, C., Kolev, V., Yordanova, J., Domschke, K., Falkenstein, M., Baune, B. T., et al. (2010). The role of BDNF Val66Met polymorphism for the synchronization of error-specific neural networks. *Journal of Neuroscience*, *30*, 10727–10733.
Beste, C., Willemssen, R., Saft, C., & Falkenstein, M. (2010). Response inhibition subprocesses and dopaminergic pathways: Basal ganglia disease effects. *Neuropsychologia*, *48*, 366–373.
Beste, C., Dziobek, I., Hielscher, H., Willemssen, R., & Falkenstein, M. (2009). Effects of stimulus–response compatibility on inhibitory processes in Parkinson's disease. *European Journal of Neuroscience*, *29*, 855–860.
Beste, C., Willemssen, R., Saft, C., & Falkenstein, M. (2009). Error processing in normal aging and in basal ganglia disorders. *Neuroscience*, *159*, 143–149.
Beste, C., Saft, C., Andrich, J., Gold, R., & Falkenstein, M. (2008a). Response inhibition in Huntington's disease—A study using ERPs and sLORETA. *Neuropsychologia*, *46*, 1290–1297.
Beste, C., Saft, C., Andrich, J., Gold, R., & Falkenstein, M. (2008b). Stimulus–response compatibility in Huntington's disease: A cognitive-neurophysiological analysis. *Journal of Neurophysiology*, *99*, 1213–1223.
Beste, C., Saft, C., Güntürkün, O., & Falkenstein, M. (2008). Increased cognitive functioning in symptomatic Huntington's disease as revealed by behavioral and event-related potential indices of auditory sensory memory and attention. *Journal of Neuroscience*, *28*, 11695–11702.
Beste, C., Saft, C., Yordanova, J., Andrich, J., Gold, R., Falkenstein, M., et al. (2007). Functional compensation or pathology in cortico-subcortical interaction in preclinical Huntington's disease. *Neuropsychologia*, *45*, 2922–2930.
Bokura, H., Yamaguchi, S., & Kobayashi, S. (2005). Event-related potentials for response inhibition in Parkinson's disease. *Neuropsychologia*, *43*, 967–975.
Cepeda, C., Wu, N., Andre, V. M., Cummings, D. M., & Levine, M. S. (2007). The corticostriatal pathway in Huntington's disease. *Progress in Neurobiology*, *81*, 253–271.
DeLong, M. R., & Wichmann, T. (2007). Circuits and circuit disorders of the basal ganglia. *Archives of Neurology*, *64*, 20–24.
Falkenstein, M., Hoormann, J., & Hohnsbein, J. (1999). ERP components in Go/Nogo task and their relation to inhibition. *Acta Psychologica*, *101*, 267–291.
Gurney, K., Prescott, T. J., Wickens, J. R., & Redgrave, P. (2004). Computational models of the basal ganglia: From robots to membranes. *Trends in Neuroscience*, *27*, 453–459.
Huntington's Disease Collaborative Research Group. (1993). An novel gene containing a trinucleotide repeat that is expanded and unstable on Huntington's disease chromosomes. *Cell*, *72*, 971–983.
Huntington Study Group. (1996). Unified Huntington's disease rating scale: Reliability and consistency. *Movement Disorders*, *11*, 136–142.
Kitano, K., & Fukai, T. (2004). Temporal characteristics of the predictive synchronous firing modeled by spike-timing dependent plasticity. *Learning and Memory*, *11*, 267–276.
Kolev, V., & Yordanova, J. (1997). Analysis of phase-locking is informative for studying event-related EEG activity. *Biological Cybernetics*, *76*, 229–235.
Lago-Fernandez, L. F., Corbacho, F. J., & Huerta, R. (2001). Connection topology dependence of synchronization of neural assemblies on class I and II excitability. *Neural Networks*, *14*, 687–696.
Langbehn, D. R., Brinkman, R. R., Falush, D., Paulsen, J. S., Hayden, M. R., & International Huntington's disease collaborative group. (2004). A new model for prediction of the age of onset and penetrance for Huntington's disease based on CAG length. *Clinical Genetics*, *65*, 267–277.
Mangun, G. R. (1995). Neural mechanisms of visual selective attention. *Psychophysiology*, *32*, 4–8.
Mitchell, I. J., Cooper, A. J., & Griffith, M. R. (1999). The selective vulnerability of striatopallidal neurons. *Progress in Neurobiology*, *59*, 691–719.
Münte, T. F., Ridao-Alonso, M. E., Preinfalk, J., Wieringa, B. M., Matzke, M., Dengler, R., et al. (1997). An electrophysiological analysis of altered cognitive functions in Huntington's disease. *Archives of Neurology*, *54*, 1089–1098.
Nguyen, L., Bradshaw, J. L., Stout, J. C., Croft, R. J., & Georgiou-Karistianis, N. (2010). Electrophysiological measures as potential biomarkers in Huntington's disease. *Brain Research Reviews*, *64*, 177–194.
Nieuwenhuis, S., Yeung, N., van den Wildenberg, W., & Ridderinkhof, K. R. (2003). Electrophysiological correlates of anterior cingulate function in a go/nogo task: Effects of response conflict and trial type frequency. *Cognitive Affective and Behavioural Neuroscience*, *3*, 17–26.
Nunez, P. L., Srinivasan, R., Westdorp, A. F., Wjiesinghe, R. S., Tucker, D. M., Silberstein, R. B., et al. (1997). EEG coherency. I: Statistics, reference electrode, volume conduction, Laplacians, cortical imaging, and interpretation at multiple scales. *Electroencephalography Clinical Neurophysiology*, *103*, 499–515.
Ocklenburg, S., Güntürkün, O., & Beste, C. (2011). Lateralized neural mechanisms underlying the modulation of response inhibition processes. *Neuroimage*, *55*, 1771–1778.
Penney, J. B., Jr., Vonsattel, J. P., MacDonald, M. E., Gusella, J. F., & Myers, R. H. (1997). CAG repeat number governs the development rate of pathology in Huntington's disease. *Annals of Neurology*, *41*, 689–692.
Perrin, F., Pernier, J., Bertrand, O., & Echalier, J. F. (1989). Spherical splines for scalp potential and current density mapping. *Electroencephaolgraphy Clinical Neurophysiology*, *72*, 184–187.
Pivik, R. T., Broughton, R. J., Coppola, R., Davidson, R. J., Fox, N., & Nuwer, M. R. (1993). Guidelines for the recording and quantitative analysis of electroencephalographic activity in research contexts. *Psychophysiology*, *30*, 547–558.
Praamstra, P., & Plat, F. M. (2001). Failed suppression of direct visuomotor activation in Parkinson's disease. *Journal of Cognitive Neuroscience*, *13*, 547–558.
Redgrave, P., & Gurney, K. (2006). The short-latency dopamine signal: A role in discovering novel actions? *Nature Reviews Neuroscience*, *7*, 967–975.
Redgrave, P., Prescott, T. J., & Gurney, K. (1999). The basal ganglia: A vertebrate solution to the selection problem? *Neuroscience*, *89*, 1009–1023.
Redgrave, P., Rodriguez, M., Smith, Y., Rodriguez-Oroz, M. C., Lehericy, S., Bergman, H., et al. (2010). Goal-directed and habitual control in the basal ganglia: Implications for Parkinson's disease. *Nature Reviews Neuroscience*, *11*, 760–772.
Roach, B. J., & Mathalon, D. H. (2008). Event-related EEG time–frequency analysis: An overview of measures and an analysis of early gamma band phase locking in schizophrenia. *Schizophrenia Bulletin*, *34*, 907–926.
Roche, R. A., Garavan, H., Foxe, J. J., & O'Mara, S. M. (2005). Individual differences discriminate event-related potentials but not performance during response inhibition. *Experimental Brain Research*, *160*, 60–70.
Rosas, H. D., Salat, D. H., Lee, S. Y., Zaleta, A. K., Pappu, V., Fischl, B., et al. (2008). Cerebral cortex and the clinical expression of Huntington's disease: Complexity and heterogeneity. *Brain*, *131*, 1057–1068.
Stout, J. C., Paulsen, J. S., Queller, S., Solomon, A. C., Whitlock, K. B., Campbell, J. C., et al. (2011). Neurocognitive signs in prodomal Huntington disease. *Neuropsychology*, *25*, 1–14.
Tabrizi, S. J., Langbehn, D. R., Leavitt, B. R., Roos, R. A., Durr, A., Craufurd, D., et al. (2009). Biological and clinical manifestation of Huntington's disease in the longitudinal TRACK-HD study: Cross-sectional analysis of baseline data. *Lancet Neurology*, *8*, 791–801.
Tallon-Baudry, C., Bertrand, O., & Fischer, C. (2001). Oscillatory synchrony between human extrastraite areas during visual short-term memory maintenance. *Journal of Neuroscience*, *21*, RC177.
Thomas, E. A., Coppola, G., Tang, B., Kuhn, A., Kim, S., Geschwind, D. H., et al. (2011). In vivo cell-autonomous transcriptional abnormalities revealed in mice expressing mutant huntingtin in striatal but not cortical neurons. *Human Molecular Genetics*, *20*, 1049–1060.
van der Hiele, K., Jürgens, C. K., Vein, A. A., Reijntjes, R. H., Witjes-Ane, M. N., Roos, R. A., et al. (2007). Memory activation reveals abnormal EEG in preclinical Huntington's disease. *Movement Disorders*, *22*, 690–695.